NASA CONTRACTOR REPORT

NASA CR-14

c.1

NASA CR-1436

MECHANICAL BEHAVIOR OF TANTALUM-BASE T-111 ALLOY AT ELEVATED TEMPERATURE

by K. D. Sheffler, J. C. Sawyer, and E. A. Steigerwald

1. Report No. NASA CR-1436	2. Government Accession No.	3. Recipient's Catalog No.
4. Title and Subtitle MECHANICAL BEHAVIOR OF TANTALUM-BASE T-111 ALLOY AT ELEVATED TEMPERATURE		5. Report Date September 1969
		6. Performing Organization Code
7. Author(s) K.D. Sheffler, J. C. Sawyer, and E. A. Steigerwald		8. Performing Organization Report No. ER-7365
9. Performing Organization Name and Address TRW Equipment Laboratories Cleveland, Ohio 44117		10. Work Unit No.
		11. Contract or Grant No. NAS 3-9439
		13. Type of Report and Period Covered Contractor Report
12. Sponsoring Agency Name and Address National Aeronautics and Space Administration Washington, D.C. 20546		
		14. Sponsoring Agency Code

15. Supplementary Notes

16. Abstract

The tantalum-base alloy T-111 (Ta-8%W-2%Hf) has been creep tested in a vacuum environment of $<1\times10^{-8}$ torr at temperatures and stresses chosen to provide approximately 1% creep in times up to 15,000 hours. Design data from five different heats are presented in the form of a Larson Miller plot for 1% creep life. Elevated temperature tension test data show a strain aging reaction in the 1400 to 2200° F (760 to 1204° C) range which produces unusual transient creep behavior. Analysis of steady state creep data show that the minimum creep rate can be described by the expression:

$$\dot{\epsilon} = 1.65\times10^{9} \left[\mathrm{Sinh}(6.6\times10^{-5}\ \sigma) \right]^{3.17} e^{\frac{-90,000}{RT}}$$

in the temperature and stress ranges of 1800 to 2600° F (982 to 1427° C) and 500 to 45,000 psi (0.34×10^{7} to 31.0×10^{7} N/m^2). These values of activation energy and stress exponent suggest that steady state creep of T-111 is governed by a diffusion controlled microcreep mechanism rather than by non-conservative dislocation motion.

17. Key Words (Suggested by Author(s))	18. Distribution Statement Unclassified - unlimited

19. Security Classif. (of this report) Unclassified	20. Security Classif. (of this page) Unclassified	21. No. of Pages 28	22. Price* $3.00

*For sale by the Clearinghouse for Federal Scientific and Technical Information
Springfield, Virginia 22151

FOREWORD

The work described in this report was performed under NASA contract NAS 3-9439. The purpose of the study was to obtain creep life data on refractory alloys for use in designing space power systems. The NASA Project Manager was Paul E. Moorhead, of the Space Power Systems Division, Lewis Research Center. The report was originally issued as TRW report ER-7365.

INTRODUCTION

The exceptional elevated temperature strength of refractory alloys makes these materials ideally suited for use in space environments, where oxidation resistance is not a governing factor. As an example, the tantalum base alloy T-111 (Ta-8%W-2%Hf) is currently considered for tubing and for radioactive isotope capsule fabrication in space electric power systems. Long time creep strength is a critical property in such applications, and since the systems will operate either in the vacuum of outer space or in metallic vapors or liquids where the partial pressure of reactive gases is extremely low, it is necessary to test candidate materials in a non-contaminating environment to generate representative design data. The purpose of this program was to develop creep data for T-111 alloy in an ultra-high vacuum of less than 1×10^{-8} torr at temperatures and stresses chosen to provide about 1% creep in times up to 15,000 hours.

EXPERIMENTAL DETAILS

Creep Test Procedures

The creep program involved testing of nominal 0.030" thick re-crystallized sheet, at temperatures ranging from 1600 to 2600°F (870 to 1427°C) and at stresses between 500 and 45,000 psi (0.34 x 10^7 to 31.0 x 10^7 N/m^2). A combination of parameters was generally selected which would provide 1% total creep in 5000 to 15,000 hours. Although specimens were normally cut with the tensile axis parallel to the rolling direction, dupli-cate tests on parallel and perpendicular samples indicated little dependence of creep strength on orientation.

Both the construction and operation of the ultra-high vacuum creep test chambers and the service instruments in the laboratory have been described in detail elsewhere (1,2). The creep test procedure involved initial evacuation of the chamber to a pressure of less than 5 x 10^{-10} torr at room temperature, followed by heating of the test specimen at such a rate that the pressure never rose above 1 x 10^{-6} torr. Pretest heat treatments were performed in situ, and complete thermal equilibrium of the specimen was insured by a two-hour hold at the test temperature prior to load application. Pressure was always below 1 x 10^{-8} torr during the tests and generally fell into the 10^{-10} torr range as testing proceeded. Specimen extension was deter-mined over a two-inch gauge length with an optical extensometer which measured the distance between two scribed reference marks to an accuracy of $\pm$50 micro-inches. Creep strains were calculated using the loaded gauge length as the original length. Specimen temperature was established at the beginning of each test using a thermocouple. An optical pyrometer having a precision of $\pm$1F° was calibrated against the thermocouple reading and was then used as the prime temperature reference throughout each test.

Characterization of Test Materials

Because the basic aim of the test program was the development of design data, several heats were tested to evaluate property variation between lots of material. Chemical analyses and room temperature mechanical properties of each heat are presented in Table I, while typical light and electron micro-graphs are shown in Figures 1 and 2A. Although the structure appears clean at optical magnifications, the electron micrographs show that T-111 recrystall-ized 1 hour at 3000°F (1649°C) has an included second phase which is distri-buted preferentially at the grain boundaries. Electron probe micrographs emphasize this grain boundary network (Figure 3), but also show a significant number of inclusions within the grains. Electron probe spectral distribution and emission scans indicate that these inclusions are hafnium oxides.

Elevated temperature tension tests were performed in a Brew furnace at pressures on the order of 10^{-5} torr at an extension rate of 0.005 in./in./min. (except where noted). The influence of temperature on the tensile properties of recrystallized T-111 is shown in Figure 4. These overlapping data from several different heats as well as from the literature (3) show a pronounced ultimate strength peak near 1400°F, together with a maximum in the strain hardening exponent. In addition, a Portevin-LeChatlier effect (serrated stress-strain curve) was observed in this temperature range, as illustrated in Figure 5. Schmidt, et al (4) have observed similar strain aging effects at a much lower temperature (about 600°F (316°C) in pure tantalum and in tantalum containing 225-955 ppm C, O, and N additions. Comparison of the T-111 data with Schmidt's results suggest that strain aging in T-111 may be caused by a complex atmosphere-dislocation interaction rather than by simple interstitial dislocation pinning. Baird and Jameson (5) have found the complex atmosphere to be a much more potent strengthener than straight-forward interstitial atom strain aging in the analogous Fe-Mn-C system, especially at higher temperatures.

In order to study the strain aging phenomenon in greater detail and perhaps identify the responsible atom species, a series of tension tests were conducted on T-111 at different strain rates and temperatures in the strain aging range. Results of these tests, shown in Figure 6, further emphasize the presence of the strain aging by showing a very large negative strain rate sensitivity in the strain aging temperature range. Two other interesting effects are also apparent in Figure 6. First, strain age strengthening is much more effective at the lower strain rates, indicating that this factor may be important in creep behavior. Second, the strength peak shifts to higher temperatures with increasing strain rate, presumably due to the more rapid diffusion required for strain aging in the faster tests. The latter behavior provides a possible method for identifying the interstitial atom species responsible for strain aging. Kinoshita (6) has pointed out that the activation energy for strain aging can be determined from the strain rate sensitivity of the strength peak by plotting strain rate vs. the reciprocal of the peak temperature. This Arrhenius type of representation which is shown in Figure 7 yields an activation energy of 22,000 cal/mole for the strain aging reaction in T-111. This value is very close to the activation energy reported by Schmidt, et al., (4,11) for diffusion of oxygen in tantalum (22,900 cal/mole) but is much lower than the values reported for diffusion of C and N in tantalum (39,600 and 41,100 cal/mole respectively). It thus seems likely that oxygen is the critical interstitial specie in the strain age strengthening of T-111.

RESULTS AND DISCUSSION

Design Considerations

Because of the low creep rates involved, conventional first stage creep was not always observed, and certain tests showed a very unusual behavior, with the creep rate first diminishing to a very low value and then increasing again to a steady state. The tendency toward this type of behavior was temperature dependent, with tests at the lower temperatures (near 0.4 Tm)* curving upward more sharply than those at higher temperatures (near 0.5 Tm) (Figure 8). The time to reach 1% creep was used to characterize the creep results for design purposes, and this property has been correlated with temperature and stress in Figure 9 using the Larson Miller parameter. A constant of fifteen was chosen to facilitate comparison of this data with other refractory alloy creep data in the literature. A satisfactory correlation was achieved in this fashion, and good agreement was found between the five heats tested.

Rationalization of the Transient Creep Behavior

Analysis of the transient creep behavior in T-111 is facilitated by plotting true strain rate vs. true strain, as illustrated in Figure 10 for the two tests shown in Figure 8. This type of plot emphasizes the fact that the upward curvature is not classical third stage creep, since the right half of the low temperature curve in Figure 10 shows a negative rather than a positive curvature. Both curves would presumably turn upward in true third stage creep if permitted to run long enough.

Comparison of the tensile and creep data on T-111 reveals that both the strain aging and the transient creep strengthening phenomenon are most pronounced at the lower test temperatures (in the 1600°F (870°C) range) and that both decrease gradually with increasing temperature and are essentially absent above about 2200°F (1204°C). This similarity of temperature dependencies suggests that the two phenomenon may be associated. Even so, it is difficult to explain why the effectiveness of a strain age strengthening mechanism should decrease with increasing test time. This phenomenon has been observed previously in an Fe-Cr-C alloy by DeBarbadillo (7), who attributed the decreasing strength to precipitation of chromium carbide. It was shown that both Cr and C were necessary by testing binary Fe-Cr and Fe-C alloys in which the unusual transient did not appear. Thus, as the chromium and carbon co-precipitated, the species necessary for strain aging was depleted from the matrix. DeBarbadillo further supported this supposition by showing that the kinetics of the precipitation reaction are such as to cause an abrupt creep rate transition of the observed form.

---

* Tm = Absolute melting temperature (°R). Since an exact melting point for T-111 alloy has not been determined, an estimated value of 5860°R was used, as reported in a product data sheet from Wah Chang Albany, a supplier of this material.

4

Examination of creep tested T-111 specimens shows that the precipitation mechanism is not directly applicable to the T-111 alloys. Figure 2B reveals an appreciable decrease rather than an increase in the number of inclusions after test. This decrease has been confirmed using the electron probe microanalyzer. It is accompanied by a significant and consistent decrease in oxygen composition, as well as a drop in tensile strength and hardness in the tested material (Table 2). Although sufficient creep tested material was not available to comprehensively evaluate the strength of the strain aging reaction in the post-tested material, a 56% decrease in the yield point drop was observed as a result of creep testing, indicating that the reaction is much weaker after creep test exposure.

It therefore seems likely that a mechanism similar to DeBarbadillos' can be proposed for T-111 alloy involving softening of the creep tested material by depletion of the species responsible for strain age strengthening (oxygen) from the matrix. Since oxygen removal proceeds during creep testing, it causes a progressive weakening and a concomitant creep rate transition at the low test temperatures where strain aging is initially an important factor.

Rationalization of Steady State Creep Behavior

Various standard analytical techniques were applied to the T-111 steady state creep data to gain better insight into the creep mechanisms involved. Neither the common engineering representation of log stress vs. log minimum creep rate nor the Arrhenius plot would adequately correlate the results, so that it was necessary to utilize a temperature compensated creep rate parameter of the form

$$\dot{\varepsilon} e^{\Delta H/RT}$$

in order to rationalize the steady data. Although the usual approach to this treatment involves the use of the Arrhenius plot to obtain the activation energy, it is possible to obtain ΔH directly through statistical evaluation of the degree of correlation between the chosen stress function and $\dot{\varepsilon} e^{\Delta H/RT}$.

Three stress functions are commonly found in the literature:

a. The power function:

$$\dot{\varepsilon} \propto \sigma^n$$

b. The exponential function:

$$\dot{\varepsilon} \propto e^{B\sigma}$$

c. And the hyperbolic sine function:

$$\dot{\varepsilon} \propto [\sinh(\alpha\sigma)]^n$$

Garofolo (8) has discussed the stress dependence of creep rate and has shown that for a number of materials tested over wide ranges of stress, the power law provides a plot of $\dot{\varepsilon}e^{\Delta H/RT}$ vs. $f(\sigma)$ which is concave upward, while the exponential law provides a plot which is concave downward. Garofolo therefor proposed the hyperbolic sine relationship to solve this problem since it approximates the power law at low stresses and the exponential law at higher stresses. Figures 11, 12, and 13 show that these general observations apply to T-111 with the hyperbolic sine law being the only relationship providing a linear correlation over the entire experimental stress range of 500 to 45,000 psi. It is interesting to note that the ultimate strength data at 1800°F (982°C), 2200°F (1204°C) and 2600°F (1427°C) all fall on the same line with the creep data in Figure 13 indicating that at these temperatures and a strain rate of 0.005 in/in/min. tensile deformation is thermally activated in T-111 alloy. It should also be noted that while the exponential and power laws do not fit the data over the entire stress range, there are limited stress ranges where each of these relationships do provide a straight line fit of the data. For example, the exponential plot in Figure 11 appears to provide a linear fit between 2.4 and 20 ksi despite the pronounced curvature over the wider stress range.

Evaluations of the straight line segments from each of the three stress representations all provided a ΔH value of about 90,000 cal./mole, which is close to the value of 100,000 cal./mole reported in the literature (11) for self diffusion in tantalum. Since lattice strains introduced by substitution of the somewhat smaller W atom in the Ta lattice probably enhance diffusivity, the apparent activation energy for creep is probably very close to that for either Ta or W diffusion in T-111. This indication of diffusion controlled creep seems somewhat surprising in view of the low homologous temperature range examined (.39 to .52); however, Sherby and Burke (9) have suggested that at very low strain rates diffusion controlled creep may occur at lower than normal temperatures as a result of the long times available for diffusion to occur, and this is probably the explanation in the present case.

Diffusion controlled creep is normally assumed to result either from non-conservative motion of jogged screw dislocations or from climb of edge dislocations. However, the stress exponent for these two processes should be near 5, as opposed to the value of about 3 observed in the present work. A value of n = 3 conforms to that predicted by Weertman (10) for glide controlled creep, implying that steady state creep in T-111 may be controlled by substitutional solute atom drag. In this case, the ΔH value reported should represent the activation energy for diffusion of W in T-111 rather than Ta in T-111. Unfortunately, no data on the diffusion of W in Ta are available in the literature to check this possibility. However, alloys which display microcreep often do not undergo primary creep, and do not exhibit a well developed substructure, both of which are consistent with the observed behavior in T-111. It therefore seems likely that steady state creep of T-111 is controlled by a microcreep mechanism in the temperature and stress ranges studied.

SUMMARY

Complex atmosphere strain aging involving oxygen and probably hafnium provides a transient strengthening in the early stages of T-111 creep tests in the 1600 to 2200°F (870 to 1204°C) range. At long test times, ultra-high vacuum removal of oxygen depletes the strain aging strengthening species from the matrix and causes a creep rate transition to occur. After the creep rate transition, steady state creep proceeds according to the relationship:

$$\dot{\varepsilon} = 1.65 \times 10^{9} \, [\sinh(6.6 \times 10^{-5}\sigma)]^{3.17} e^{-90,000/RT}$$

where the values of activation energy and stress exponent suggest that steady state creep is governed by a diffusion controlled microcreep mechanism.

REFERENCES

1. J.C. Sawyer, "Design and Operation of Ultra-High Vacuum Creep Equipment", <u>Transactions of the 1965 Vacuum Metallurgy Conference</u>, L.M. Bianchi, Ed. American Vacuum Society, Boston, 1965.

2. J.C. Sawyer and E.A. Steigerwald, "Creep Properties of Refractory Metal Alloys in Ultra-High Vacuum", Journal of Materials, Vol. 2 (1967), p. 341.

3. F.F. Schmidt and H.R. Ogden, "The Engineering Properties of Tantalum and Tantalum Alloys", DMIC Report 189, September 13, 1963.

4. F.F. Schmidt, et al., WADD Technical Report 59-13, AD No. 236-957, March 1960.

5. J.D. Baird and A. Jamieson, "Effects of Manganese and Nitrogen on the Tensile Properties of Iron in the Range of 20-600°C", JISI, V. 204, p. 793, August 1966.

6. S. Kinoshita, P.J. Wray, and G.T. Horne, "Some Observations on the Portenin-LeChatlier Effect in Iron", Trans. AIME, Vol. 233, p. 1902, October 1965.

7. J.J. Debarbadillo, "The Effect of Substitutional Alloying Elements on the Elevated Temperature Mechanical Properties of Alpha Iron", Ph.D. Thesis, Lehigh University, 1967.

8. F. Garofalo, <u>Fundamentals of Creep and Creep-Rupture in Metals</u>, MacMillan, New York, 1965.

9. O.D. Sherby and P.M. Burke, "Mechanical Behavior of Crystalline Solids at Elevated Temperature", Progress in Material Science, Vol. 13, 1968, p. 325.

10. J. Weertman, "Creep of Indium, Lead, and Some of their Alloys with Various Metals", Trans. AIME Vol. 218, 1960, p. 207.

11. F.F. Schmidt, "Tantalum and Tantalum Alloys", DMIC Report 133, July 25, 1960.

TABLE 1

CHEMICAL COMPOSITION AND ROOM TEMPERATURE MECHANICAL PROPERTIES OF T-111 ALLOYS ANNEALED 1 HOUR AT 3000°F (1649°C)

| Heat No. | Weight Percent | | | PPM | | | MECHANICAL PROPERTIES | | |
	W	Hf	C	N_2	O_2	H_2	UTS KSI	0.2% Y.S. KSI	% Elongation
70616	8.5	2.3	.0044	20	55	6	*	*	*
65079	8.7	2.3	.0030	50	130	4	94.0	72.0	35.2
65076	8.6	2.0	.0040	20	100	3	93.2	79.9	31.0
D-1102	7.9	2.3	.0030	34	20	3	*	*	*
D-1670	7.9	2.4	.0010	20	72	<5	*	*	*
D-1183	8.7	2.2	.0036	10	25	6	94.3	81.0	32.8
650028	8.3	2.1	.0030	12	30	1.9	83.8	77.8	30.1
848001	7.9	2.0	.0010	13	21	1	79.3	70.0	30.7
650038	8.6	2.0	.0025	20	100	2.8	92.1	76.8	29.8

* Not Available

6

TABLE 2

EFFECT OF CREEP EXPOSURE ON ROOM TEMPERATURES MECHANICAL PROPERTIES AND COMPOSITION
OF T-111 ANNEALED ONE HOUR AT 3000°F PRIOR TO CREEP TESTING.

	CREEP TEST CONDITIONS				Before After Creep Testing	Ultimate Tensile Strength KSI	Percent Elongation	Diamond Pyramid Hardness	COMPOSITION				
									Percent		PPM		
Test No.	Heat No.	Stress KSI	Temperature °F	Test Duration Hours					Hf	C	N_2	O_2	H_2
S-26	D-1670	17	1800	1624	Before				2.17	.001	20	72	5
					After	***	***	***	2.09	.0032	30	10	5
S-31*	65079	5	2200	6602	Before	94.0	35.0						
					After	85.3	8.2+	***	***	***	**	**	**
S-33	65076	8	2200	2976	Before	93.1	31.0	247	1.95	.004	20	100	3
					After	85.7	39.0	228	2.07	.004	30	20	31
S-32	D-1102	5	2200	4322	Before				2.28	.003	34	20	3
					After	***	***	***	2.17	.003	30	10	24
S-35	65079	5	2200	5522	Before			275	2.30	.003	50	130	4
					After	***	***	257	2.14	.0046	30	10	5
S-43	65079	18	2000	361	Before				2.30	.003	50	130	4
					After	***	***	***	1.33	.003	40	10	31

+ Reduced Gauge Width
* Perpendicular to rolling direction
*** Not Available
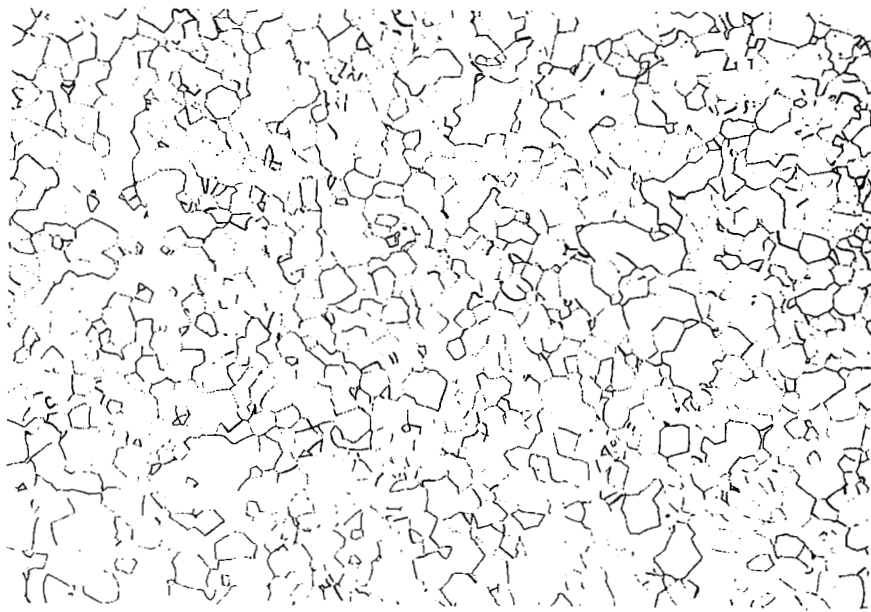
100X
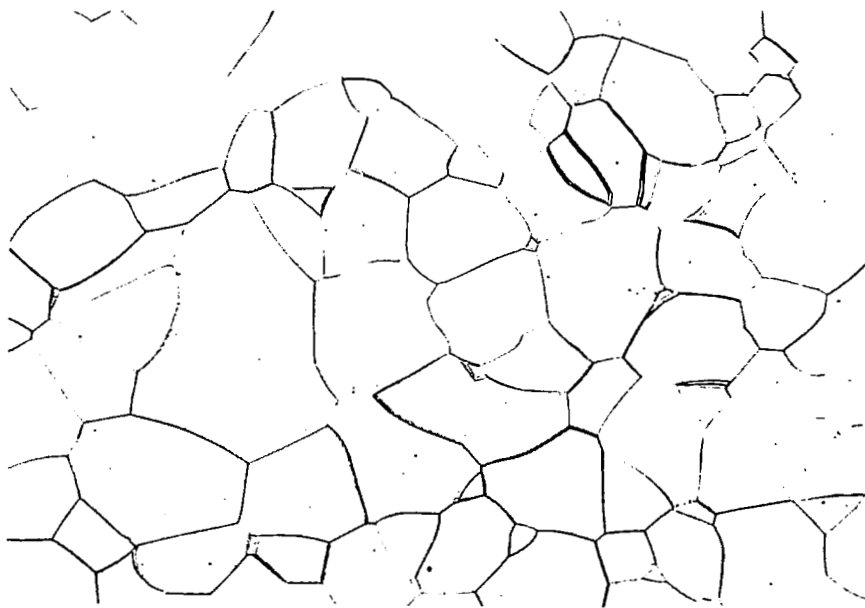
500X

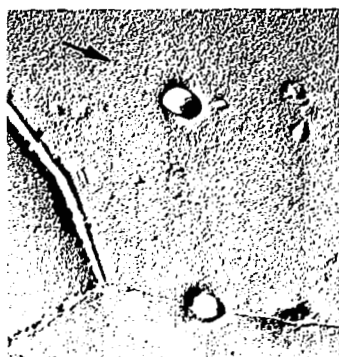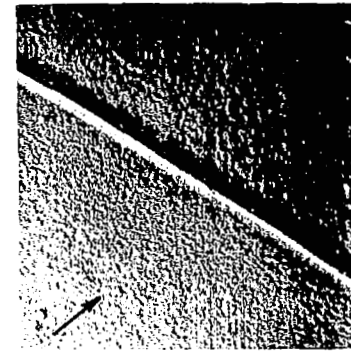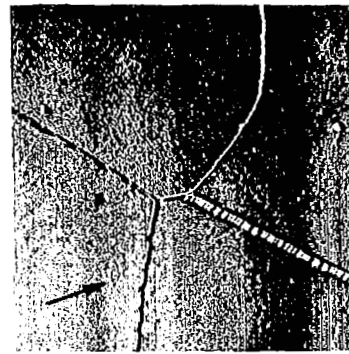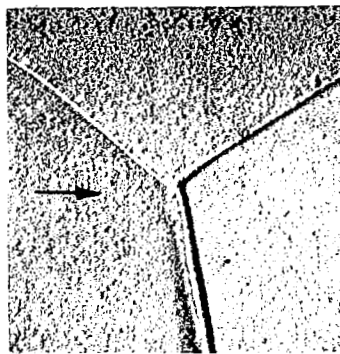FIGURE 1. OPTICAL PHOTOMICROGRAPHS OF T-111 HEAT NO. 70616 RECRYSTALLIZED
1 HOUR AT 3000°F (1649°C).

A. BEFORE CREEP TESTING
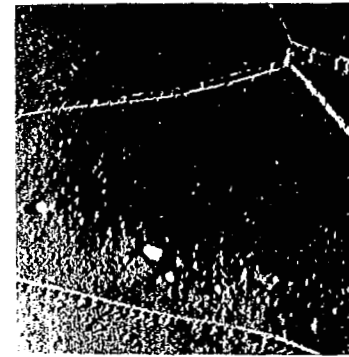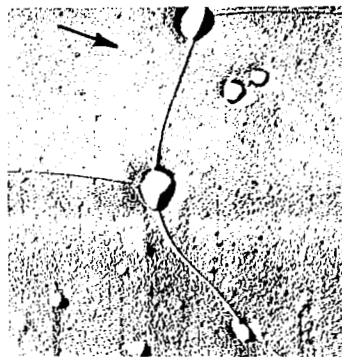

B. AFTER CREEP TESTING

Specimen S-40
Tested 8717 hours
at 1800°F (982°C)
and 17 KSI (11.7x10^7
N/M^2) Total creep
strain 1.028%
Heat No. D-1102

Specimen S-26
Tested 9624 hours
at 1800°F (982°C)
and 17 KSI (11.7x10^7
N/M^2) Total creep
strain 1.030%
Heat No. D-1670

Specimen S-33
Tested 2976 hours
at 2200°F (1204°C)
and 8 KSI (5.51x10^7
N/M^2) Total creep
strain 1.048%
Heat No. 65076

Specimen S-35
Tested 5522 hours
at 2200°F (1204°C)
and 5 KSI (3.44x10^7
N/M^2) Total creep
strain 1.092%
Heat No. 65079

FIGURE 2. ELECTRON MICROGRAPHS OF TANTALUM T-111 ALLOY (TA-8%W-2%HF) RECRYSTALLIZED 1 HOUR AT 3000°F, BEFORE AND AFTER CREEP TESTING AT THE INDICATED TEST CONDITIONS. TOTAL CHAMBER PRESSURE LESS THAN 1x10^{-8} TORR. 7500X, REDUCED 55% FOR REPRODUCTION. TWO STAGE REPLICAS (CELLULOSE-NITRATE/CARBON). ARROWS INDICATE THE DIRECTION OF CHROMIUM SHADOWING ON PRIMARY REPLICA.
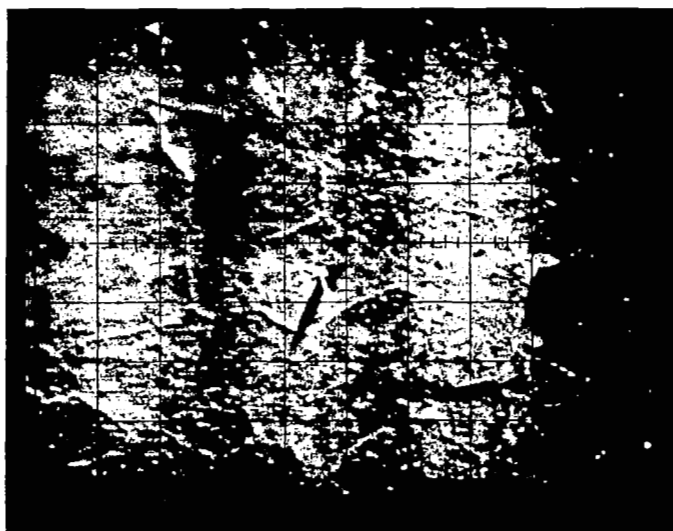
550X
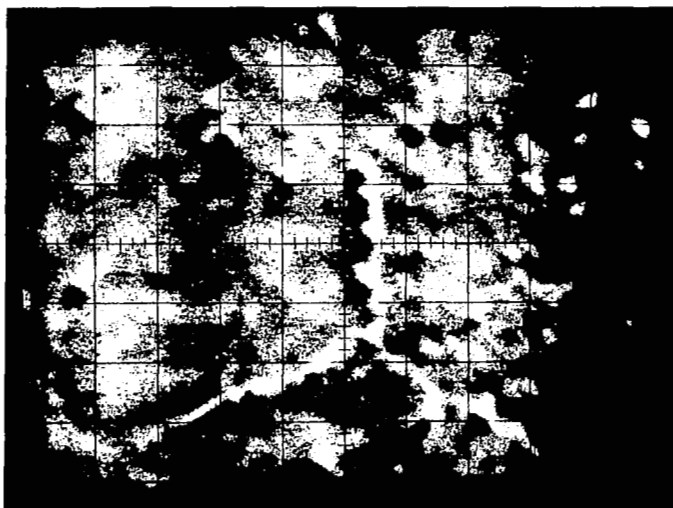
1650X

FIGURE 3. ELECTRON MICROPROBE ANALYZER CURRENT IMAGES OF T-111 HEAT D-1102 RECRYSTALLIZED 1 HOUR AT 3000°F (1649°C). BRIGHT SPOTS REPRESENT INCLUDED SECOND PHASE PARTICLES.
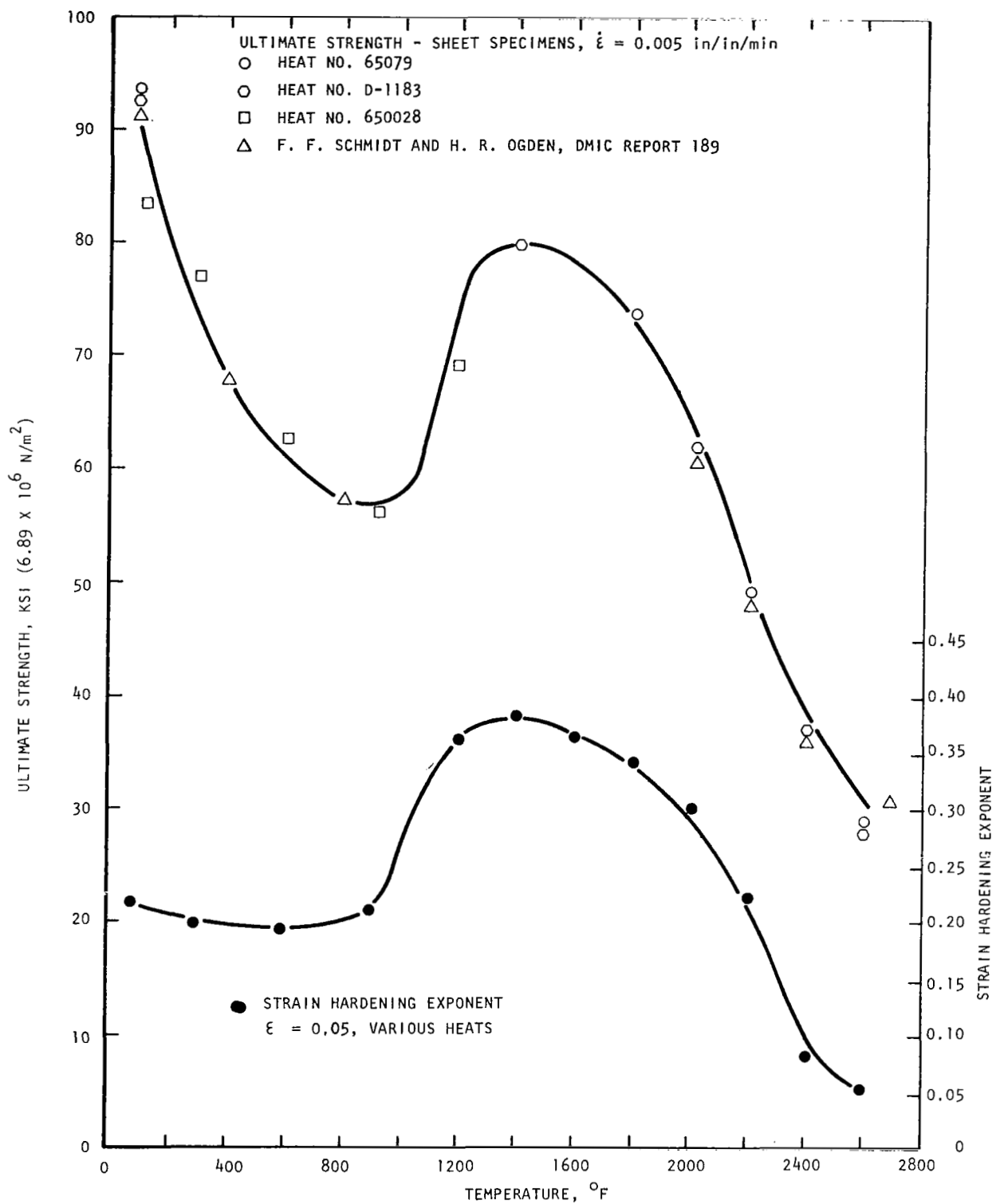
FIGURE 4a. VARIATION OF ULTIMATE STRENGTH AND STRAIN HARDENING EXPONENT
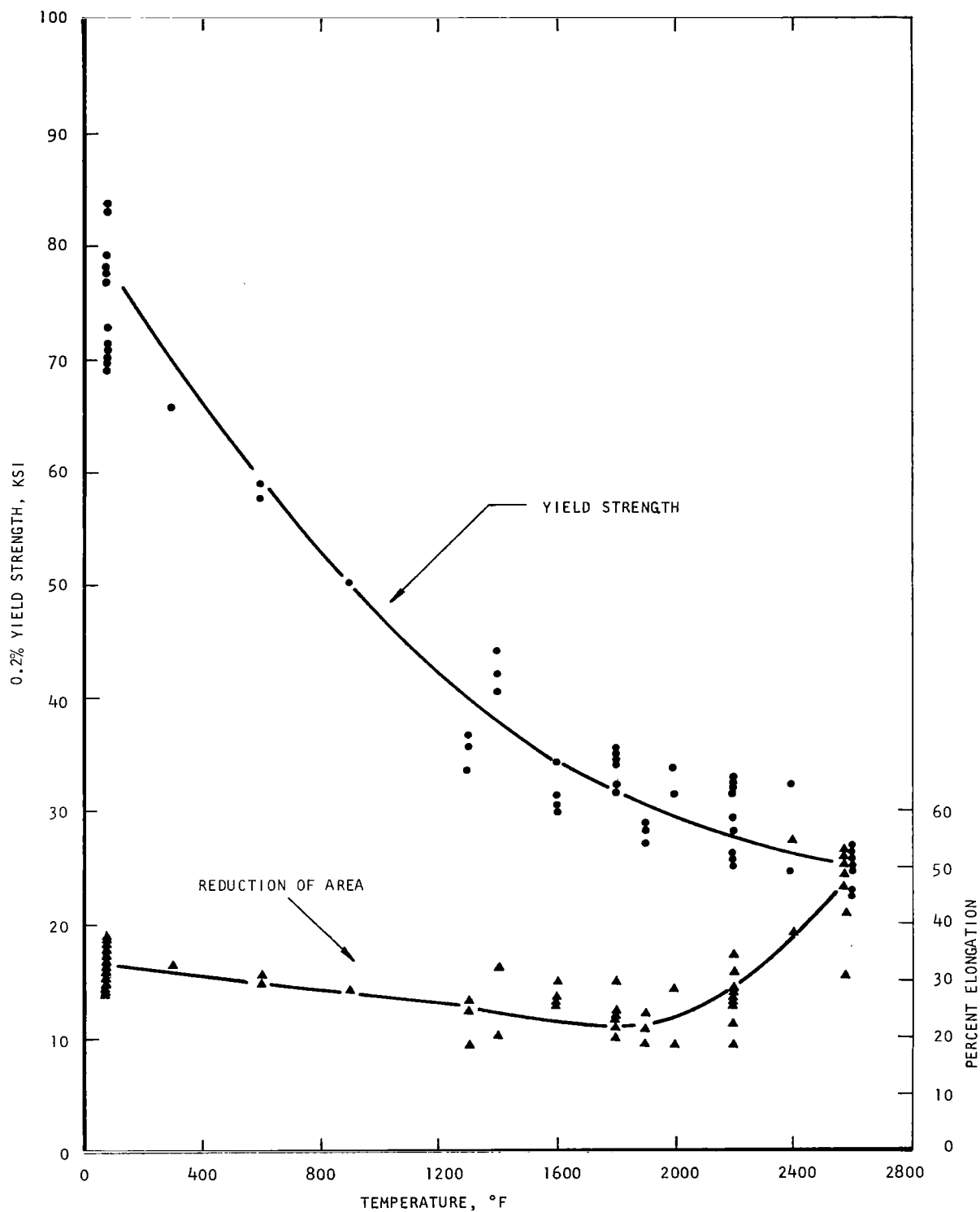WITH TEMPERATURE IN T-111 ANNEALED 1 HOUR AT 3000°F (1649°C)

FIGURE 4b.   VARIATION OF 0.2% YIELD STRENGTH AND PERCENT ELONGATION
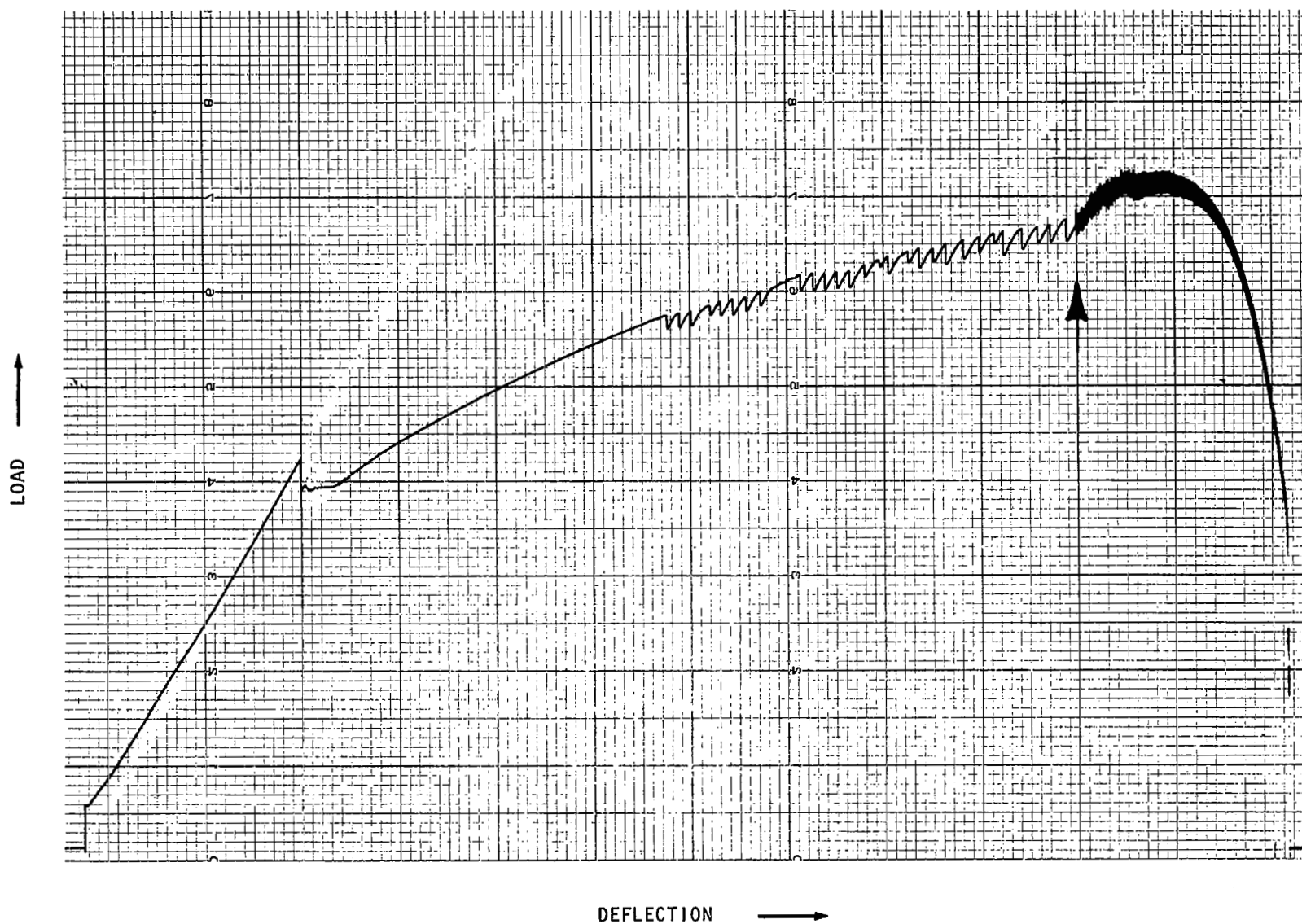WITH TEMPERATURE IN T-111 ANNEALED 1 HOUR AT 3000°F (1649°C)

FIGURE 5.   LOAD-DEFLECTION CURVE OR RECRYSTALLIZED T-111 AT
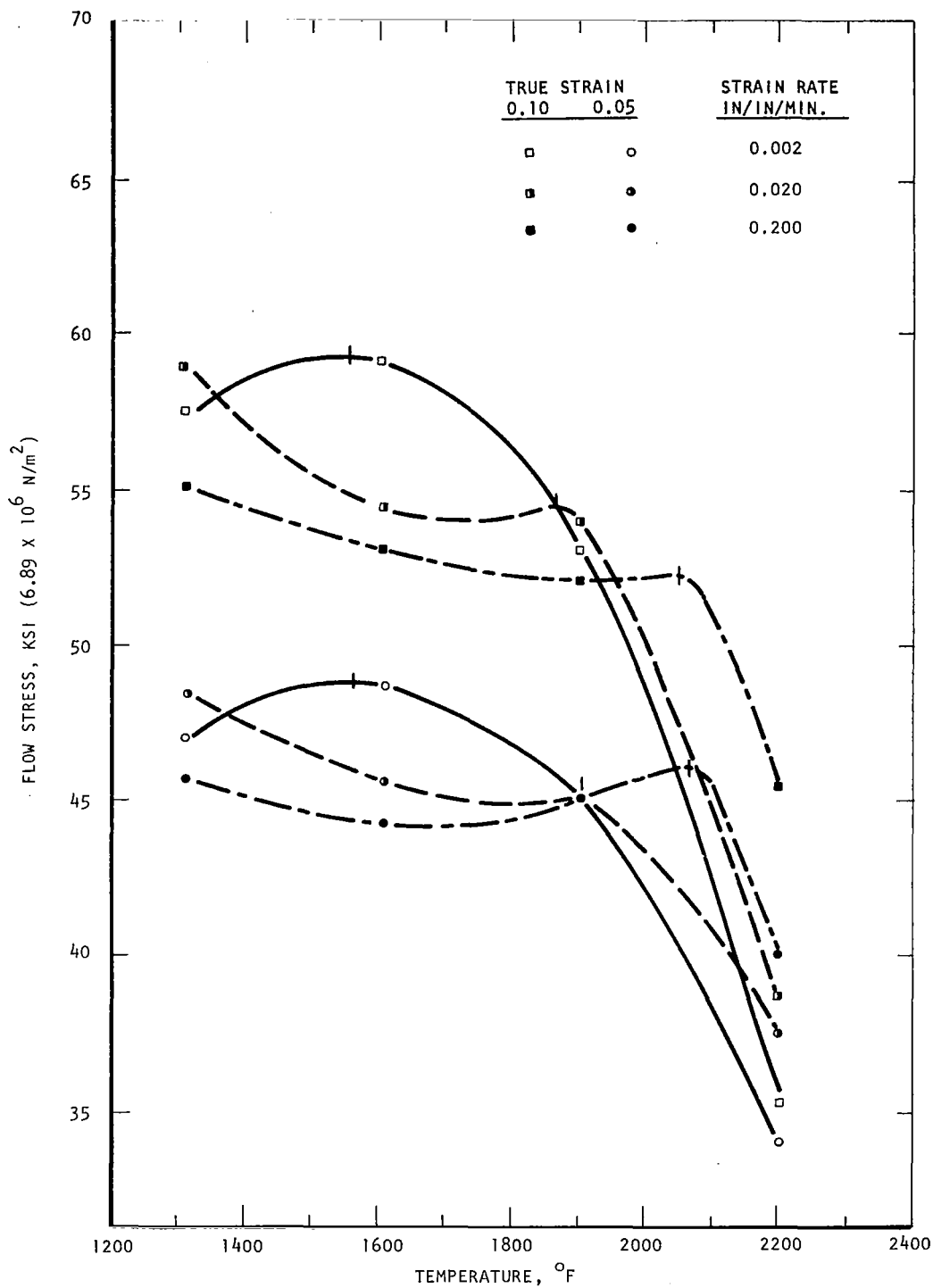   1400°F. ARROW INDICATES DECREASE OF CHART SPEED.

FIGURE 6. VARIATION OF FLOW STRESS WITH TEMPERATURE AND STRAIN RATE AT TWO LEVELS OF TRUE STRAIN IN T-111 ANNEALED 1 HOUR AT 3000°F (1649°C). TIC MARK ON EACH CURVE INDICATES STRAIN AGING PEAK.
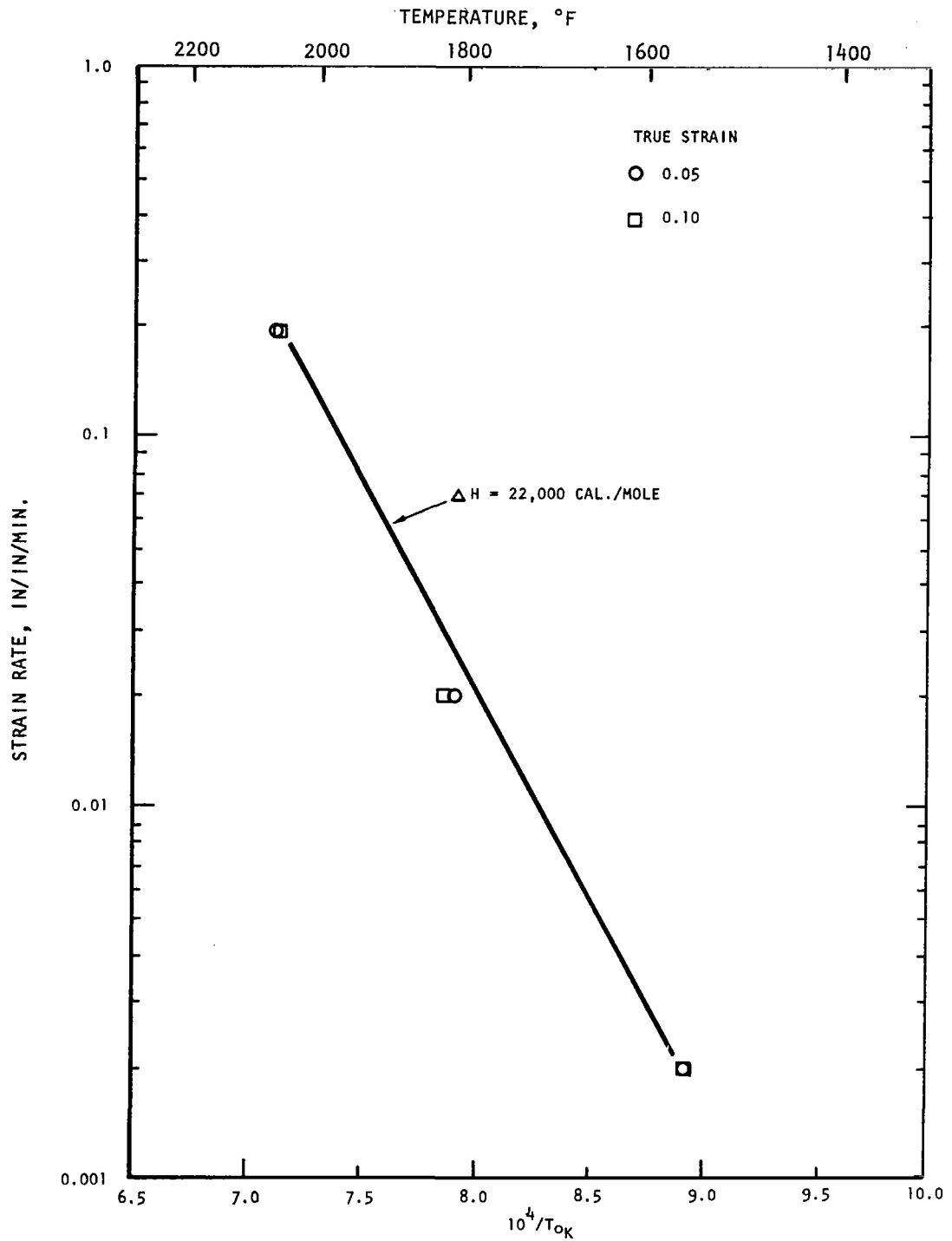
FIGURE 7. VARIATION OF STRAIN AGING PEAK TEMPERATURE WITH STRAIN RATE AT TWO LEVELS
OF TRUE STRAIN IN T-111 ANNEALED 1 HOUR AT 3000°F (1649°C). SLOPE OF
THE LINE REPRESENTS THE ACTIVATION ENERGY FOR THE STRAIN AGING.
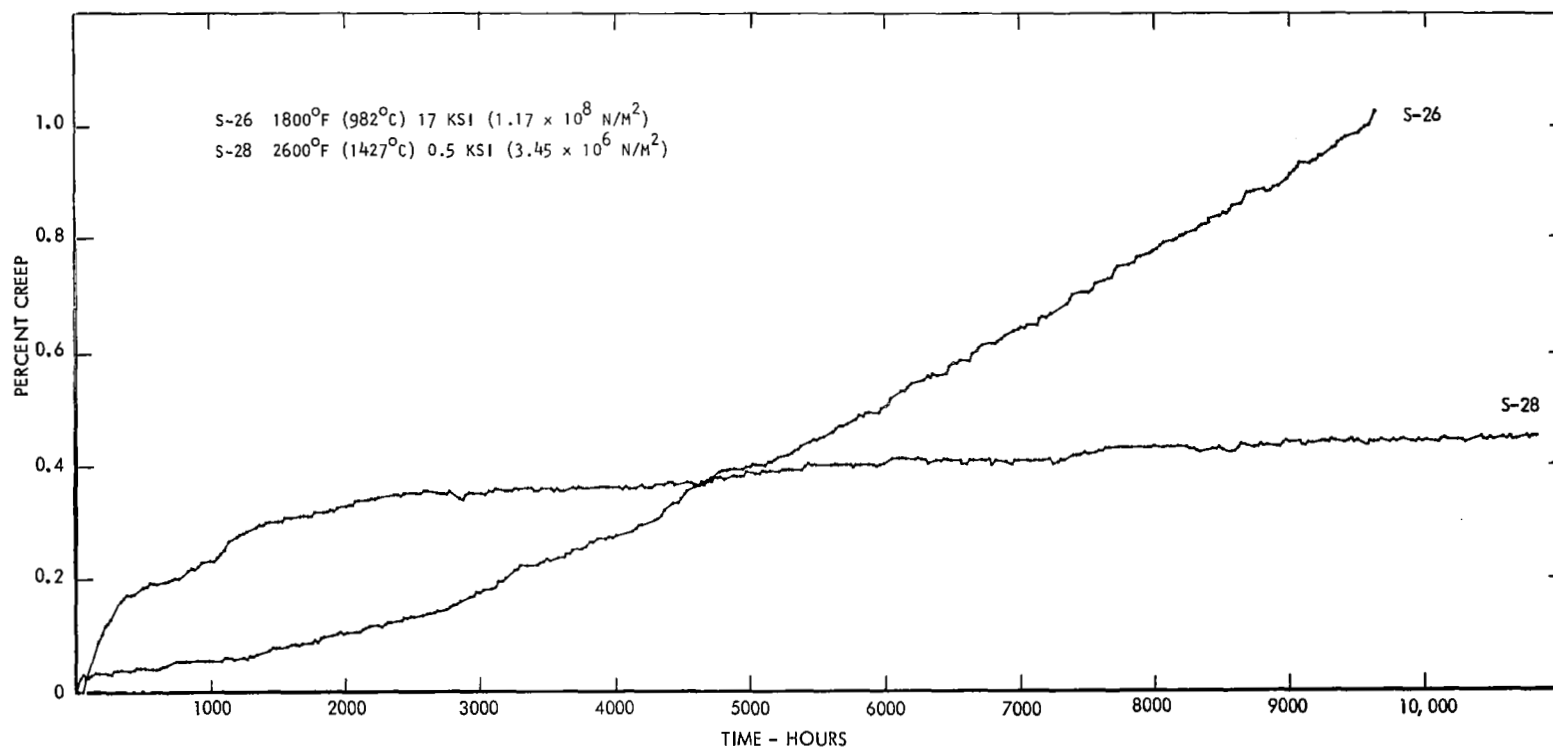
18

FIGURE 8.   CREEP TEST DATA, T-111 HEAT D-1670, ANNEALED 3000°F (1649°C)
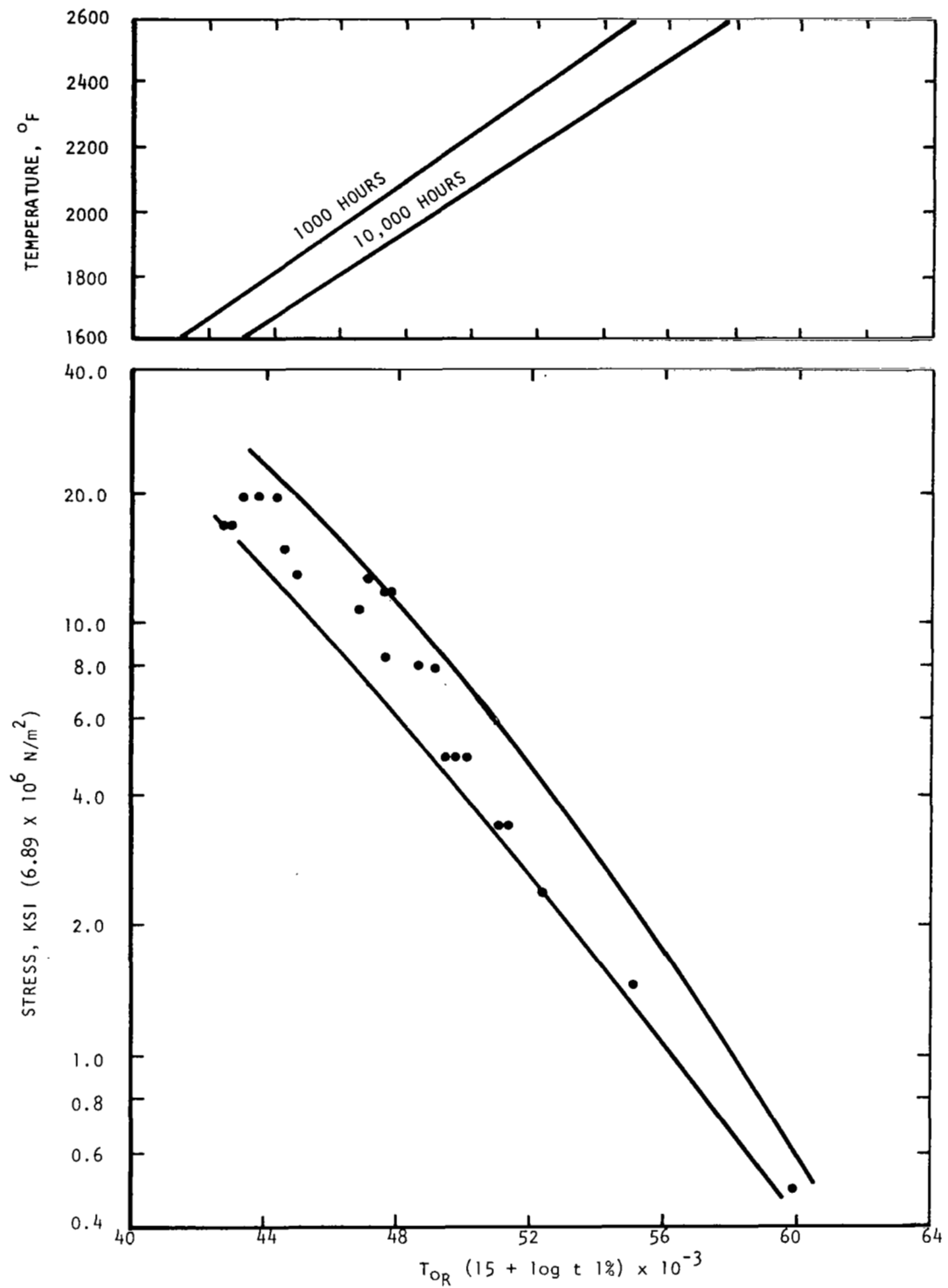1 HOUR, AND TESTED IN VACUUM ENVIRONMENT <1 x 10^{-8} TORR.

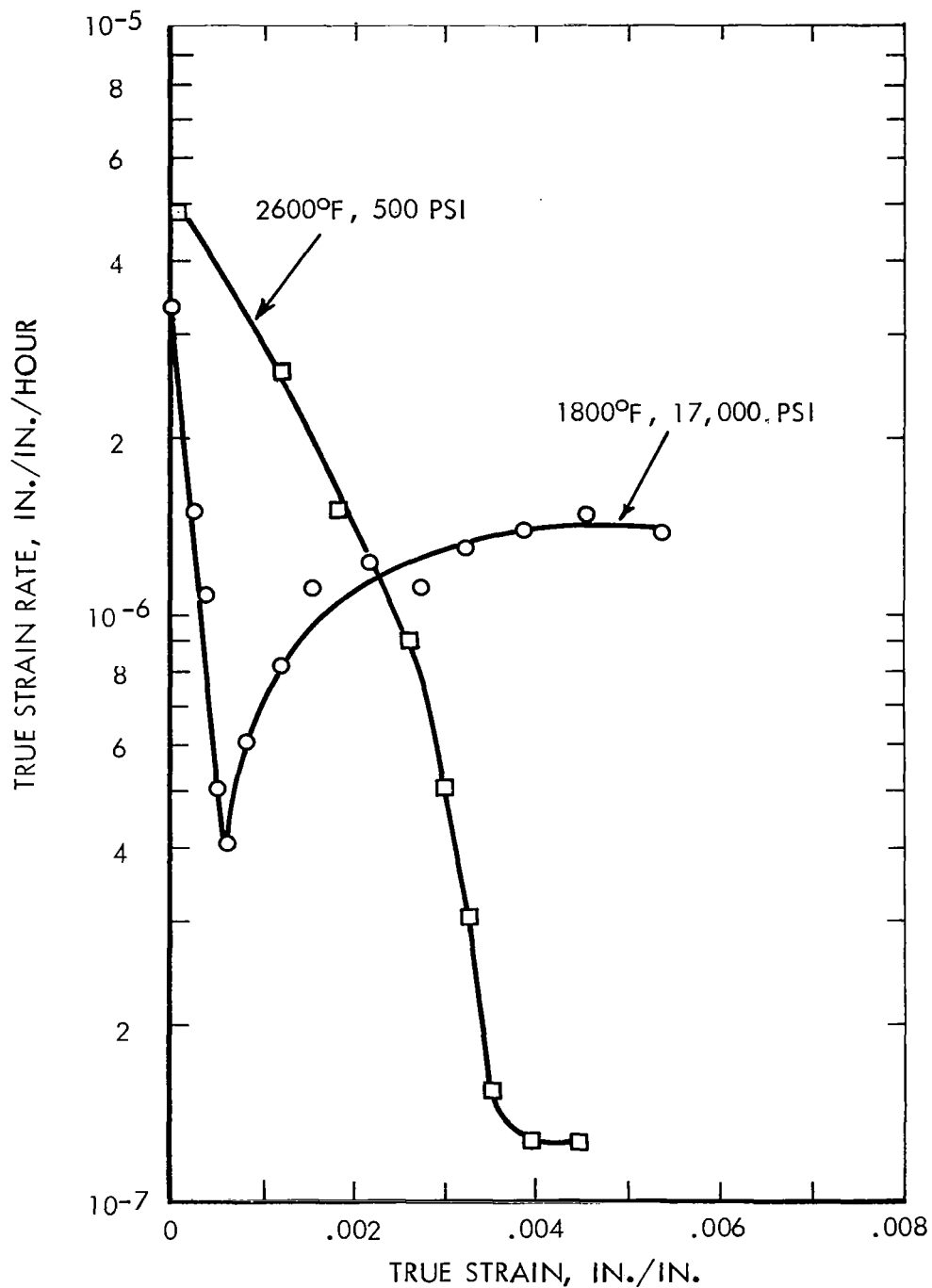FIGURE 9. LARSON MILLER PLOT OF 1% CREEP LIFE DATA FOR T-111 ALLOY ANNEALED 1 HOUR AT 3000°F (1649°C).

FIGURE 10. TRUE STRAIN RATE AS A FUNCTION OF TRUE STRAIN IN T-111
ANNEALED 1 HOUR AT 3000°F (1649°C) AND CREEP TESTED AT
THE INDICATED CONDITIONS.

21

$\dot{\varepsilon}e^{\Delta H/RT}$, $\Delta H = 90,000$ CAL./MOLE

STRESS, KSI $(6.89 \times 10^6$ N/m$^2)$

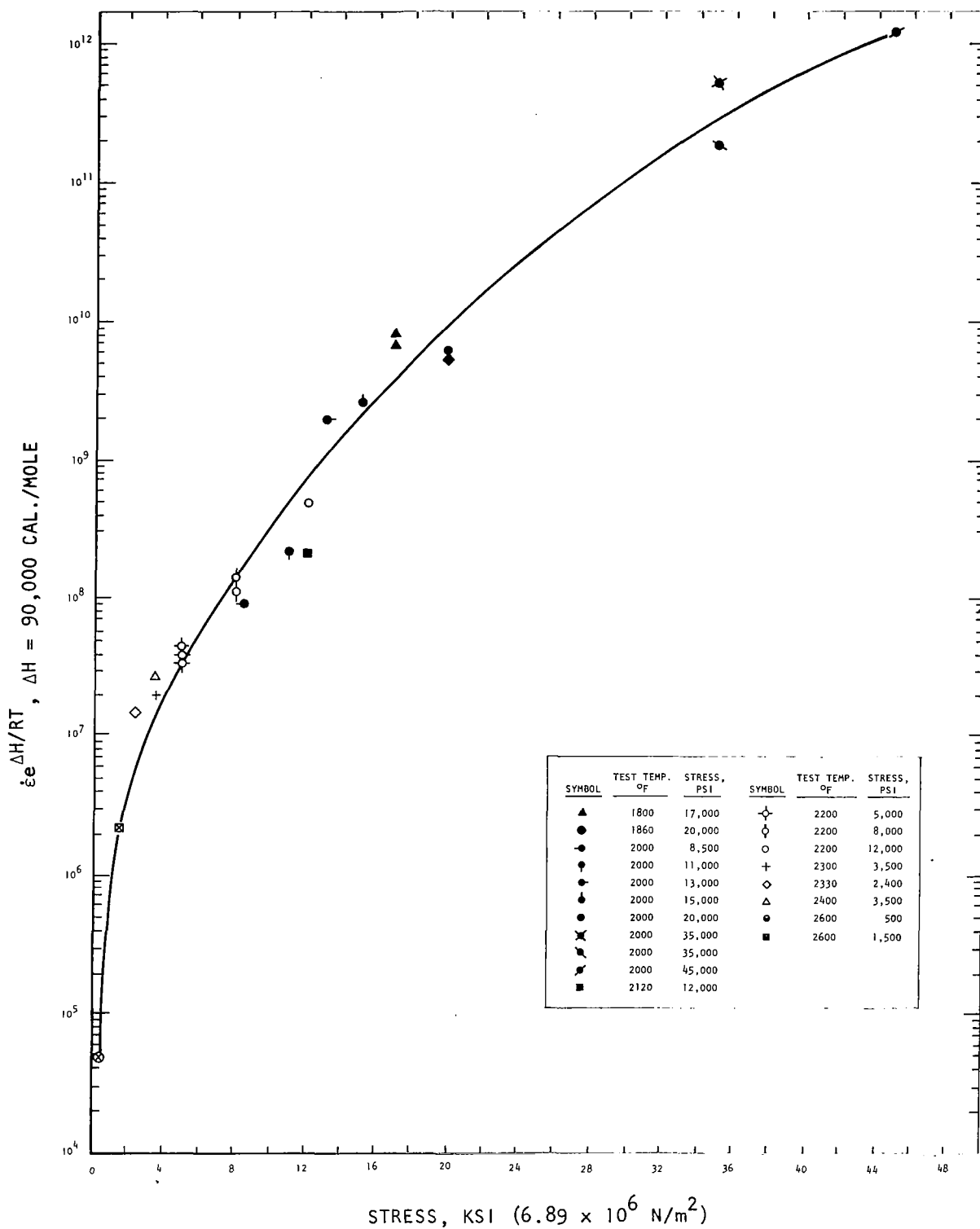| SYMBOL	TEST TEMP. °F	STRESS, PSI	SYMBOL	TEST TEMP. °F	STRESS, PSI
▲	1800	17,000	✦	2200	5,000
●	1860	20,000	◊	2200	8,000
●	2000	8,500	○	2200	12,000
●	2000	11,000	+	2300	3,500
●	2000	13,000	◇	2330	2,400
●	2000	15,000	△	2400	3,500
●	2000	20,000	●	2600	500
✕	2000	35,000	■	2600	1,500
	2000	35,000			
	2000	45,000			
■	2120	12,000			

FIGURE 11. VARIATION OF TEMPERATURE COMPENSATED TRUE STRAIN RATE WITH STRESS IN T-111 ALLOY ANNEALED ONE HOUR AT 3000°F (1649°C).

SYMBOL	TEST TEMP. °F	STRESS, PSI
▲	1800	17,000
●	1860	20,000
⦿	2000	8,500
⬤	2000	11,000
●̶	2000	13,000
▲	2000	15,000
●	2000	20,000
✕	2000	35,000
✖	2000	35,000
▰	2000	45,000
■	2120	12,000
◇̶	2200	5,000
◌̶	2200	8,000
○	2200	12,000
+	2300	3,500
◇	2330	2,400
△	2400	3,500
●	2600	500
⊠	2600	1,500

Y-axis: $\dot{\varepsilon}e^{\Delta H/RT}, \Delta H = 90{,}000$ CAL./MOLE
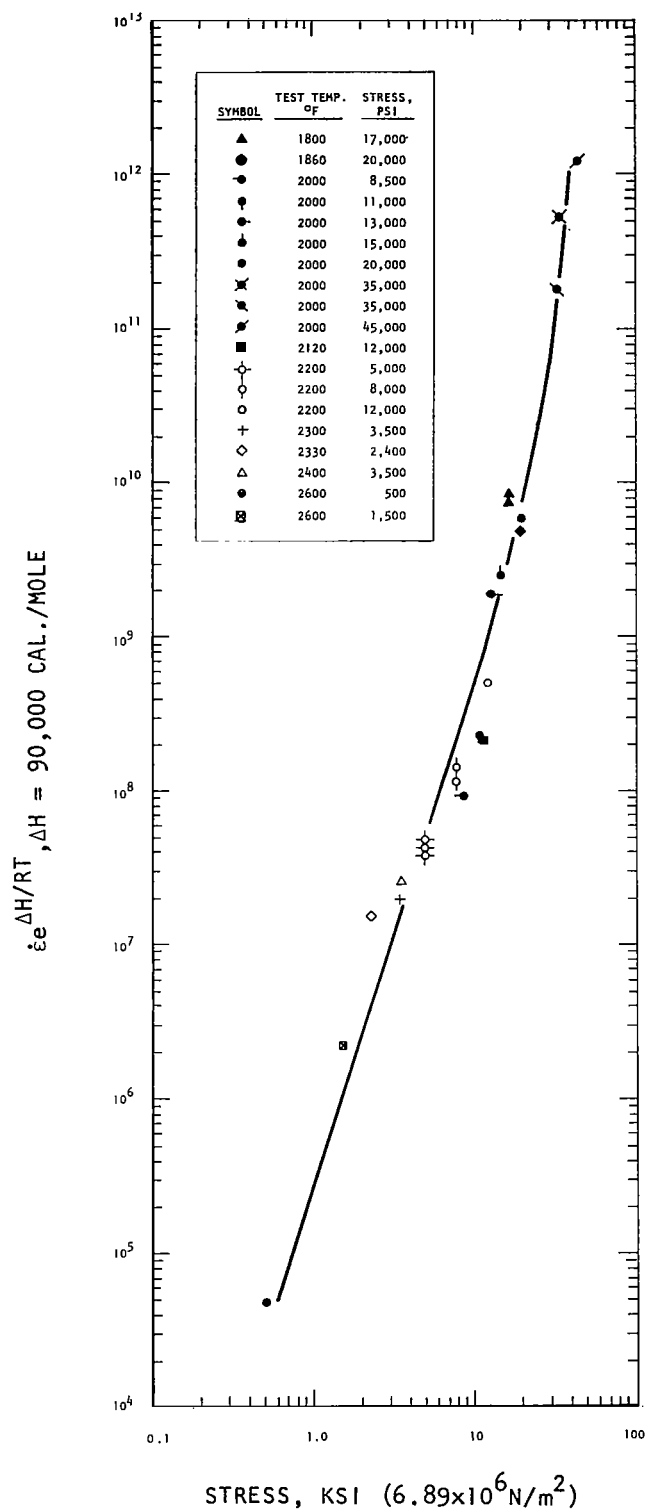
X-axis: STRESS, KSI $(6.89 \times 10^6 \text{N/m}^2)$

FIGURE 12. VARIATION OF TEMPERATURE COMPENSATED TRUE STRAIN RATE WITH LOG STRESS FOR T-111 ALLOY ANNEALED ONE HOUR AT 3000°F (1.649°C).

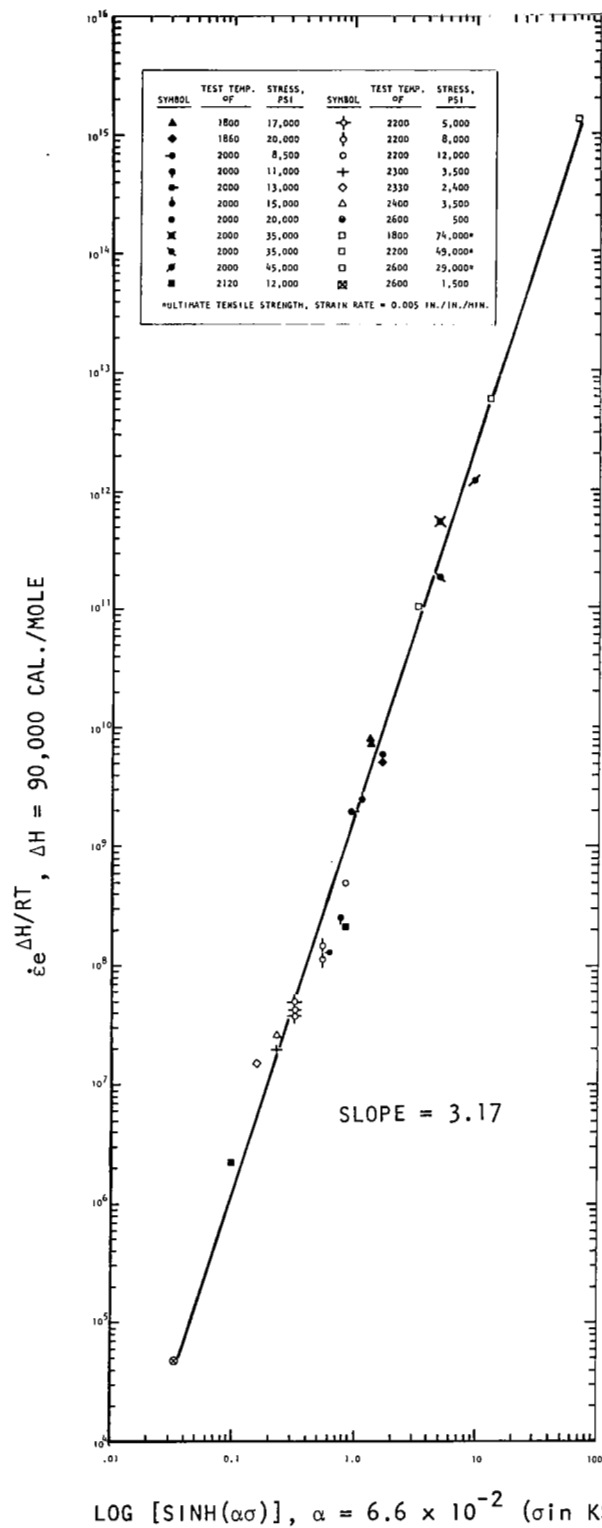FIGURE 13. VARIATION OF TEMPERATURE COMPENSATED TRUE STRAIN RATE WITH LOG [SINH $(\alpha\sigma)]^n$ IN T-111 ALLOY ANNEALED 1 HOUR AT 3000°F (1649°C).